Zastosowanie analizy modalnej do oceny degradacji sztywności połączeń w konstrukcjach prętowych

Bartłomiej Błachowski

IPPT PAN

Seminarium IPPT PAN, 7 czerwca 2010 roku

Plan prezentacji

1. Wprowadzenie
2. Cel pracy
3. Przykłady złożonych konstrukcji prętowych
4. Rodzaje połączeń stosowanych w kratownicach
5. Założenia o przegubowym łączeniu prętów
6. Weryfikacja założeń statycznych dla 25 prętowca
7. Przykład numeryczny identyfikacji sztywności węzłów prefabrykowanych
8. Modelowanie podatności połączeń w wysokich masztach
9. Procedury numeryczne do analizy dynamicznej konstrukcji prętowych o węzłach podatnych
10. Podsumowanie

Wprowadzenie

Aktualną tematyką prac wielu ośrodków badawczych na świecie jest monitorowanie stanu technicznego konstrukcji z zamiarem wykrywania jej uszkodzeń.

W tym celu proponowane są różne podejścia:

- ***Prof. Holnicki*** *(ZTI IPPT)* z zespołem - „Metoda dystorsji wirtualnych", prace eksperymentalne *dr Kołakowski*
- ***Prof. Uhl*** *(Kraków AGH)* – eksperymentalna analiza modalna
- ***Prof. Spencer*** *(USA)* – doświadczalna weryfikacja metody „Damage Locating Vectors" autorstwa *prof.Bernala*

i wiele innych

Cel pracy

Jednym z problemów niedokładnie rozpoznanych jest monitorowanie uszkodzeń w węzłach konstrukcji.

Celem pracy jest opracowanie metody oceny degradacji sztywności połączeń w konstrukcjach prętowych z uwzględnieniem rzeczywistej postaci węzłów.

Examples of lattice structures

A large number of structures are build of system of rods (beams) commonly called trusses, frames and lattice structures.

Truss bridges

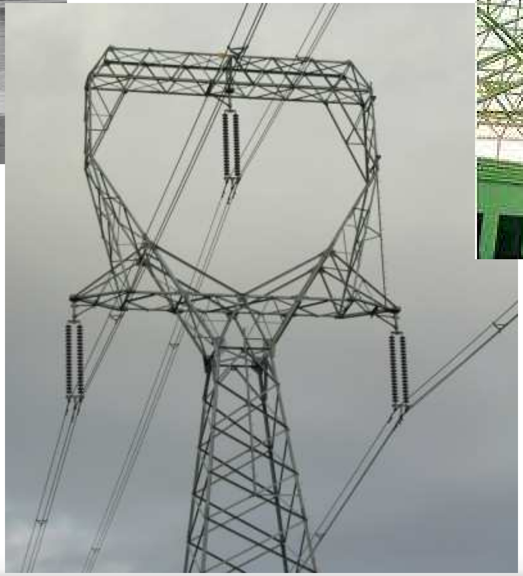

Transmission towers

Double layer grids

Joints in lattice structures

In most cases in such structures elements are rigidly connected.

FF-System
Free form

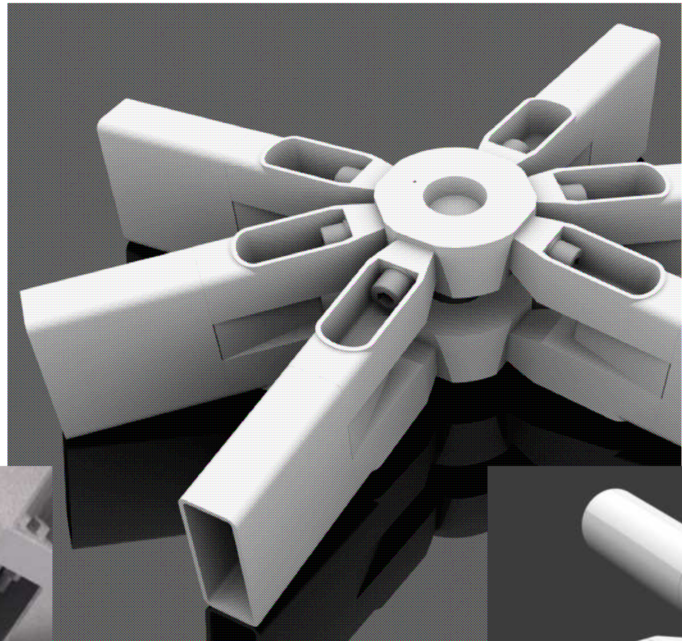

Novum System
Products

Classical welded joint

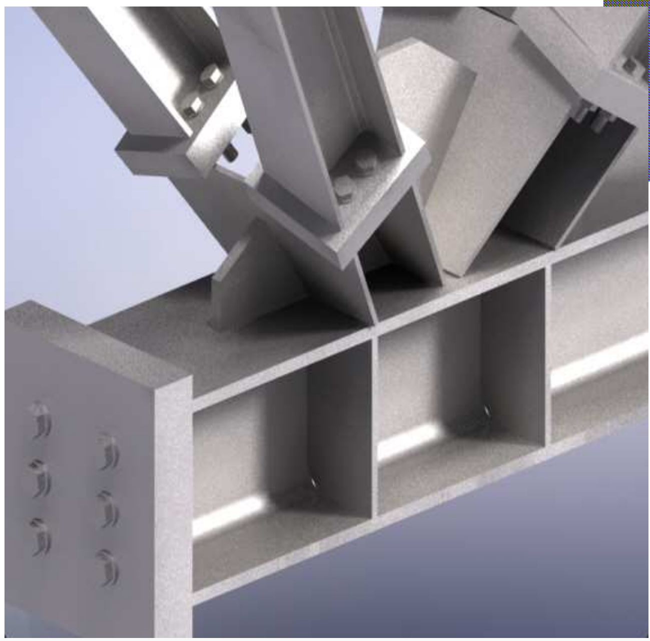

KK-System
Kugel
knoten

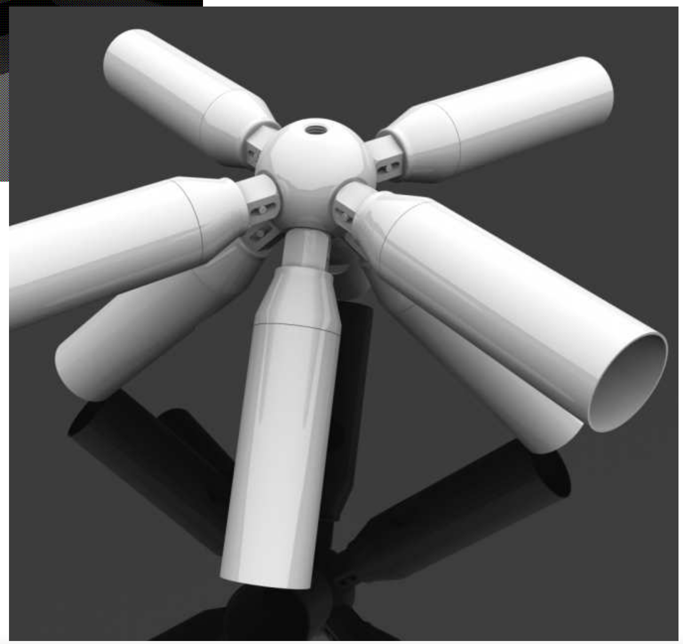

Pin-joint assumption

The origin of the „pin joint" assumption

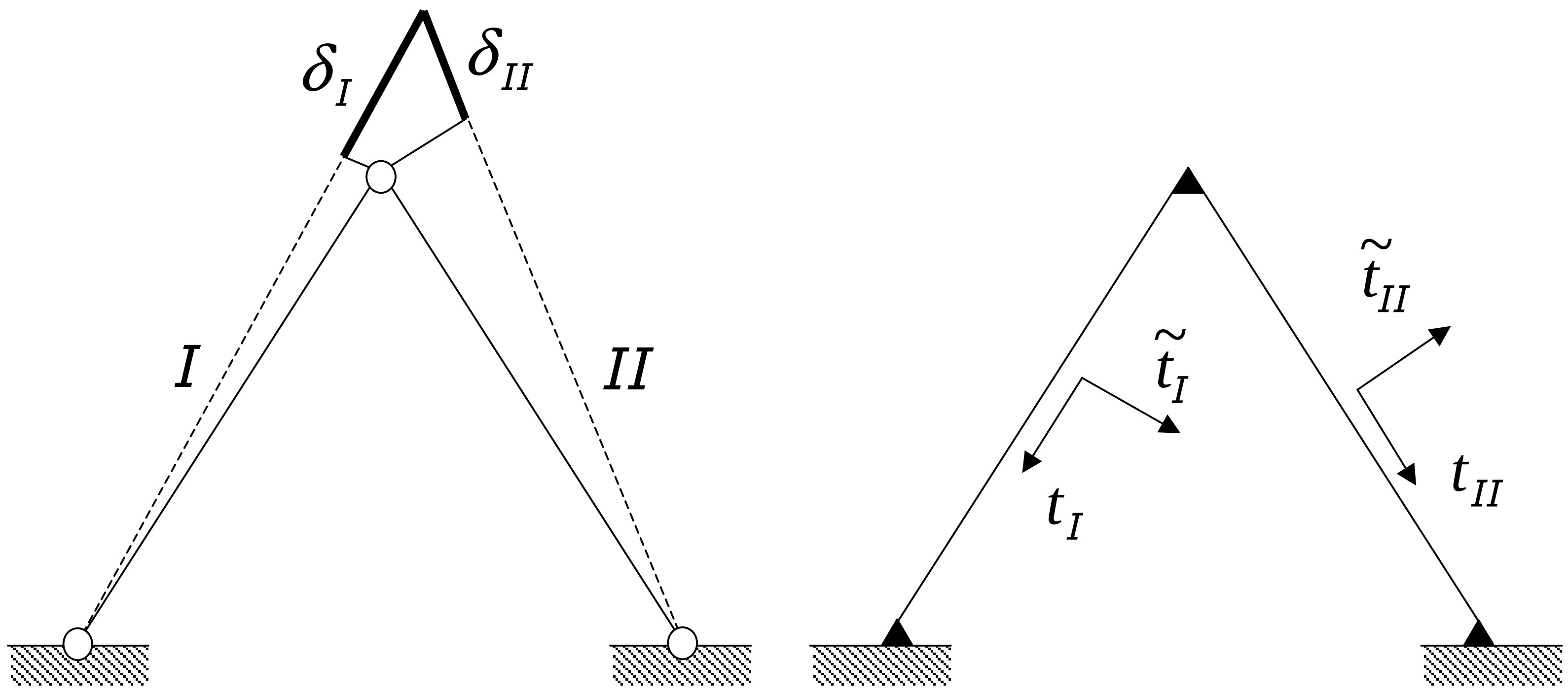

Equilibrium equation

- for pin joint

$$\begin{cases} C_I t_{I_1} \delta_I + C_{II} t_{II_1} \delta_{II} = P_1 \\ C_I t_{I_2} \delta_I + C_{II} t_{II_2} \delta_{II} = P_2 \end{cases}$$

$$C_I = \frac{EA_I}{l_I}$$

- for rigid connection

$$\begin{cases} -\tilde{K}_I \tilde{t}_{I_1} \tilde{\kappa}_I + C_I t_{I_1} \delta_I - \tilde{K}_{II} \tilde{t}_{II_1} \tilde{\kappa}_{II} + C_{II} t_{II_1} \delta_{II} = P_1 \\ -\tilde{K}_I \tilde{t}_{I_2} \tilde{\kappa}_I + C_I t_{I_2} \delta_I - \tilde{K}_{II} \tilde{t}_{II_2} \tilde{\kappa}_{II} + C_{II} t_{II_2} \delta_{II} = P_2 \\ \tilde{K}_I \vartheta_I + \tilde{K}_{II} \vartheta_{II} = 0 \end{cases}$$

$$\tilde{K}_I = \frac{EI_I}{l_I^3}$$

$$\frac{C}{\tilde{K}} = \frac{EA}{EI} l^2 = \left(\frac{l}{i} \right)^2 \rightarrow 10^4$$

Pin-joint assumption continued

When

$$t_{I_1}\delta_I \quad \text{and} \quad \tilde{t}_{I_1}\tilde{\kappa}_I$$

are of the same order then the product

$$\tilde{K}_I\tilde{t}_{I_1}\tilde{\kappa}_I$$

can be neglected comparing with $C_I t_{I_1}\delta_I$

$$\tilde{K}_I\tilde{t}_{I_1}\tilde{\kappa}_I <<< C_I t_{I_1}\delta_I$$

Neglecting bending term is equivalent to the assumption that two elements are „pin joint".

Pin-joint assumption continued

For structures when displacements are caused by bending only, „pin joint” assumption can not be applied.

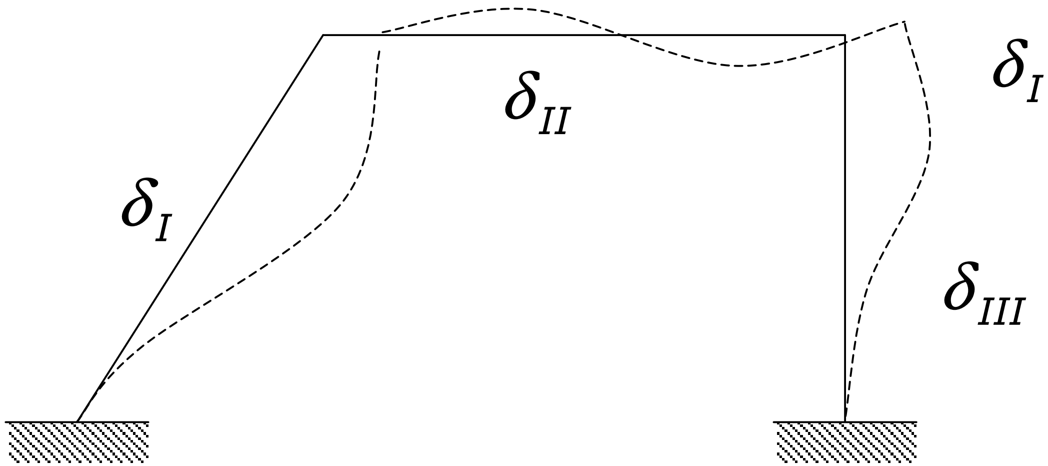

$$\delta_I = \delta_{II} = \delta_{III} = 0$$

Pin-joint assumption in dynamics

The static „pin joint" assumption has been incorporated in truss dynamics.

Equivalent masses of beams are attached to pin joints. Problem is reduced to vibration of concentrated masses connected with massless springs.

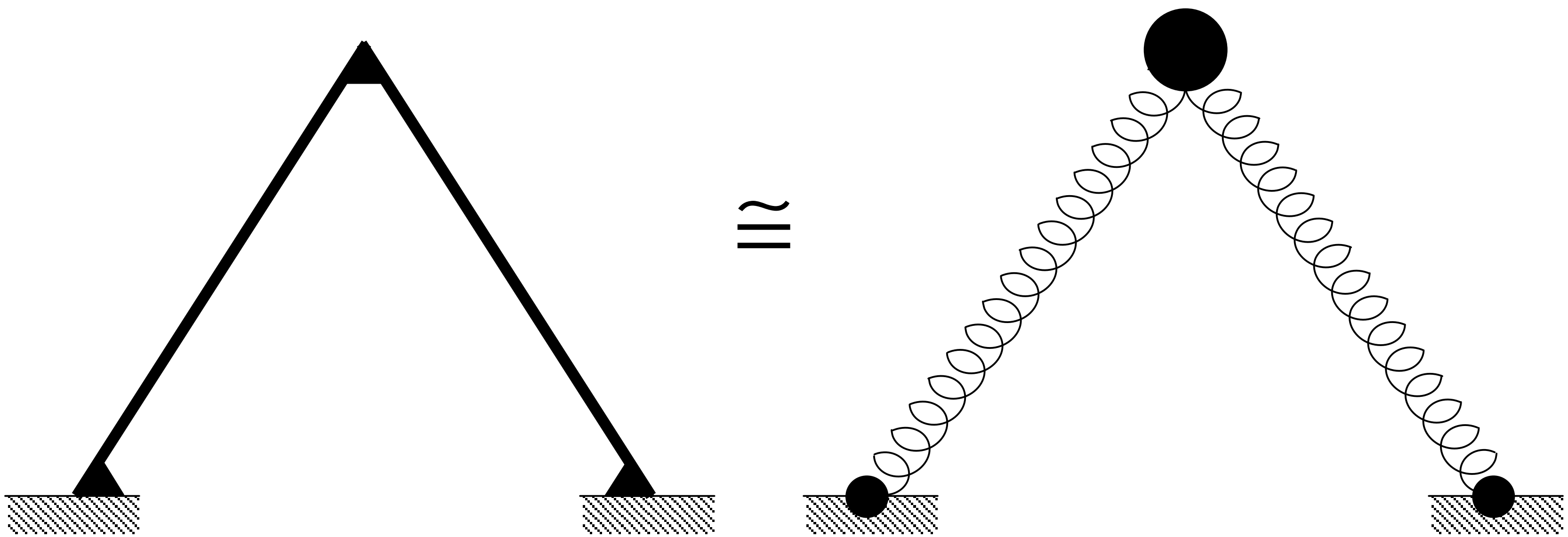

Rigidly connected structure

In real, rigidly connected structure, beam mass is distributed along its length and transversal motion assumed.

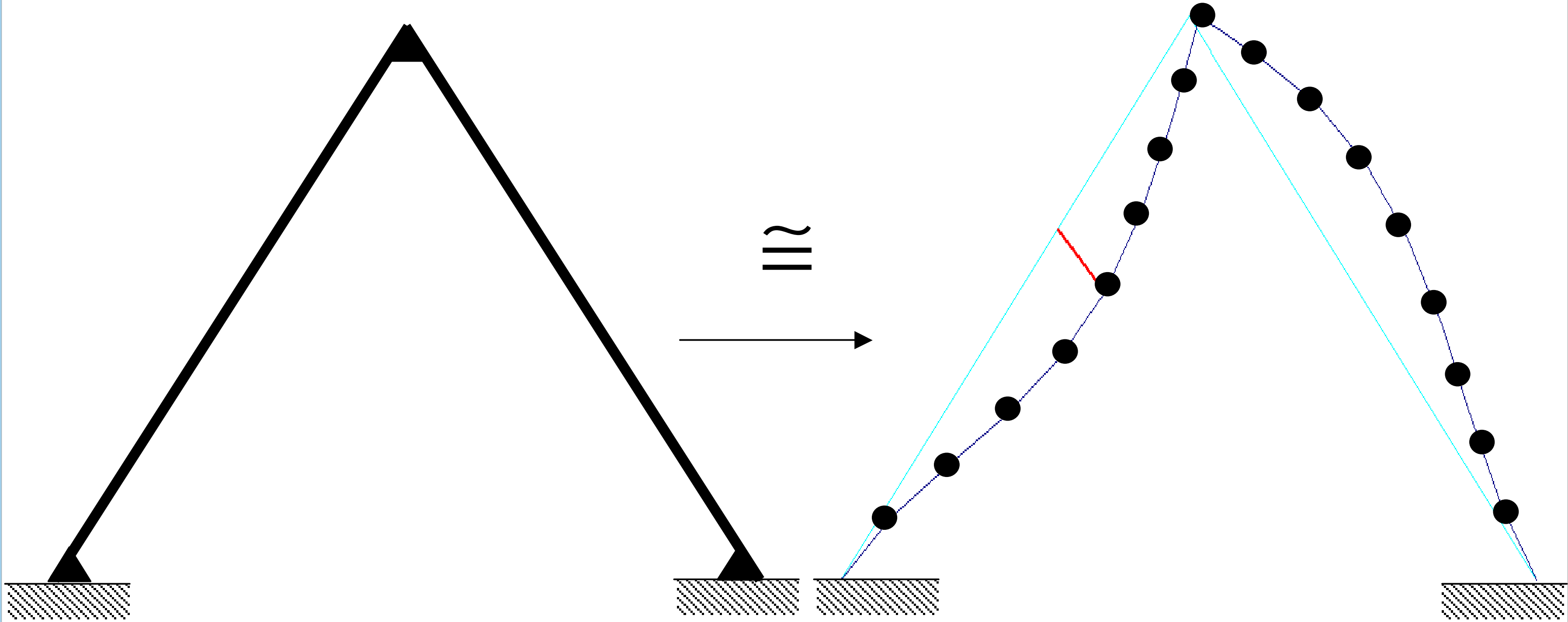

First eigenfrequency for 2 bar structure

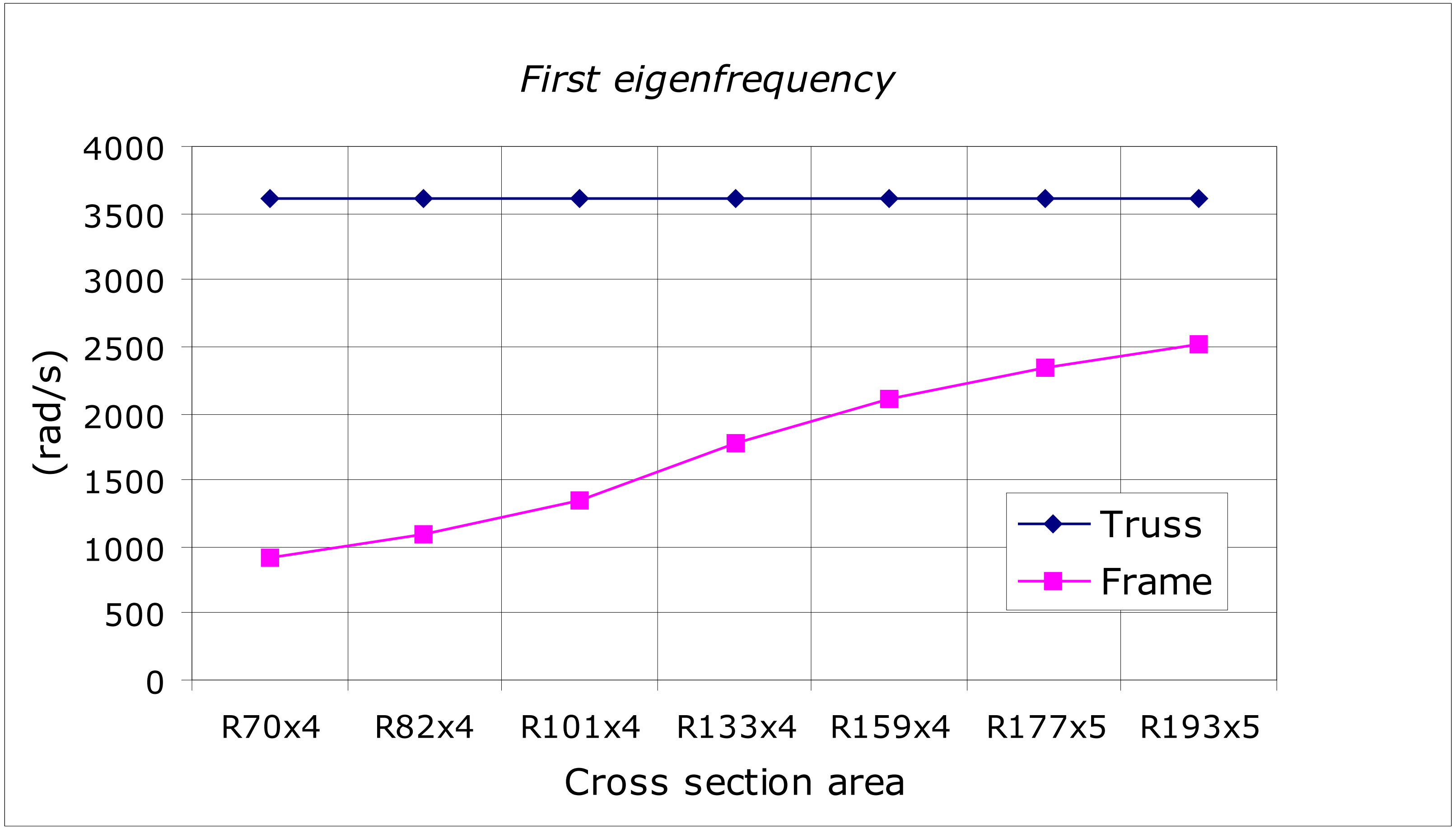

Modal analysis – 25 bar structure

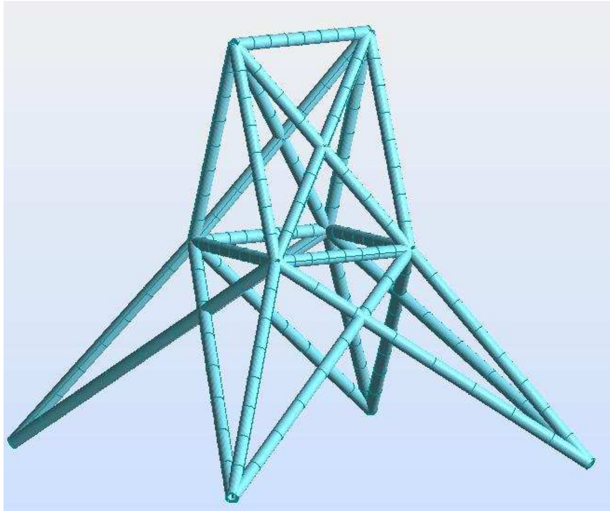

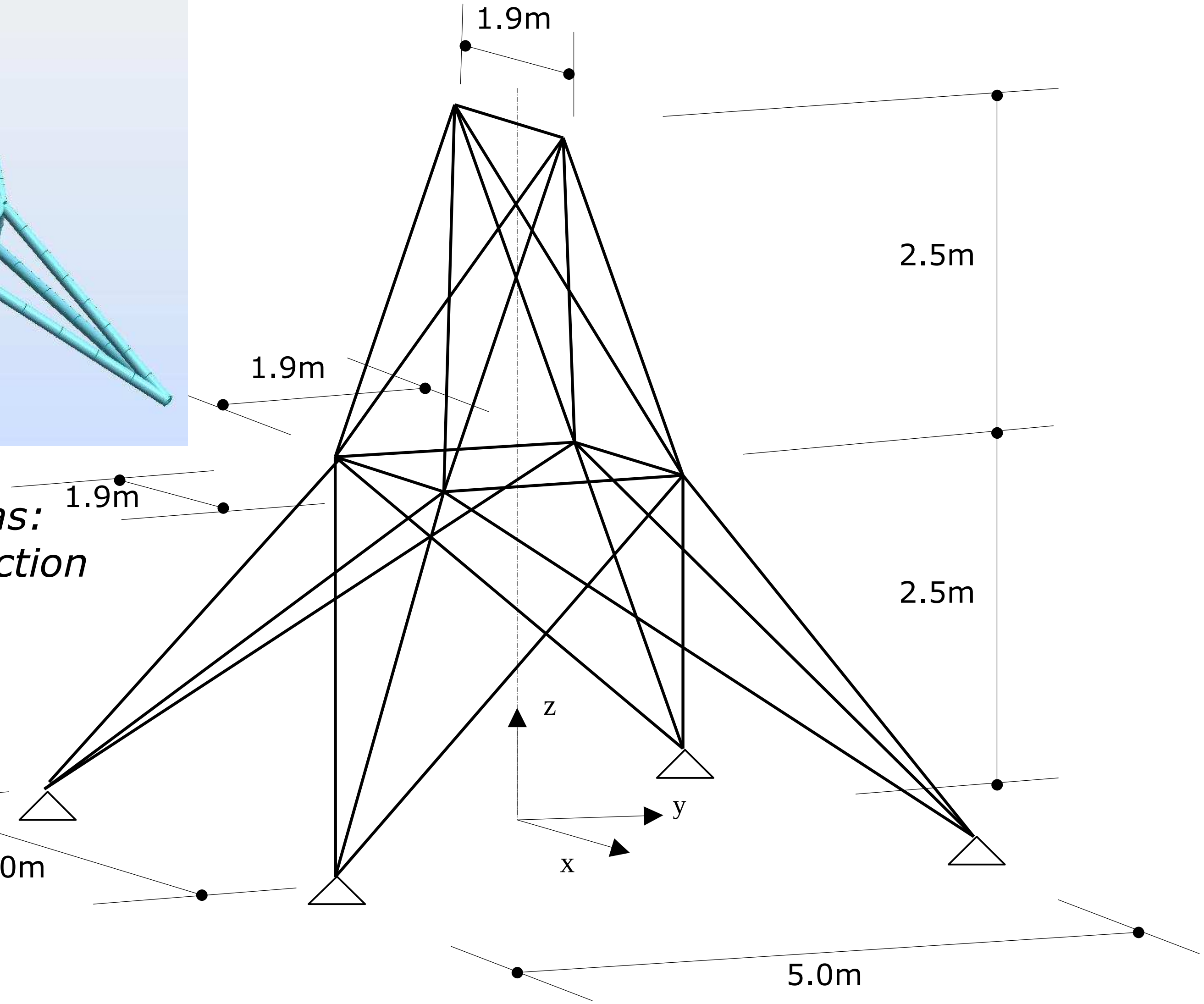

Cross section areas:
Circular hollow section
Ø159x8

First mode shape

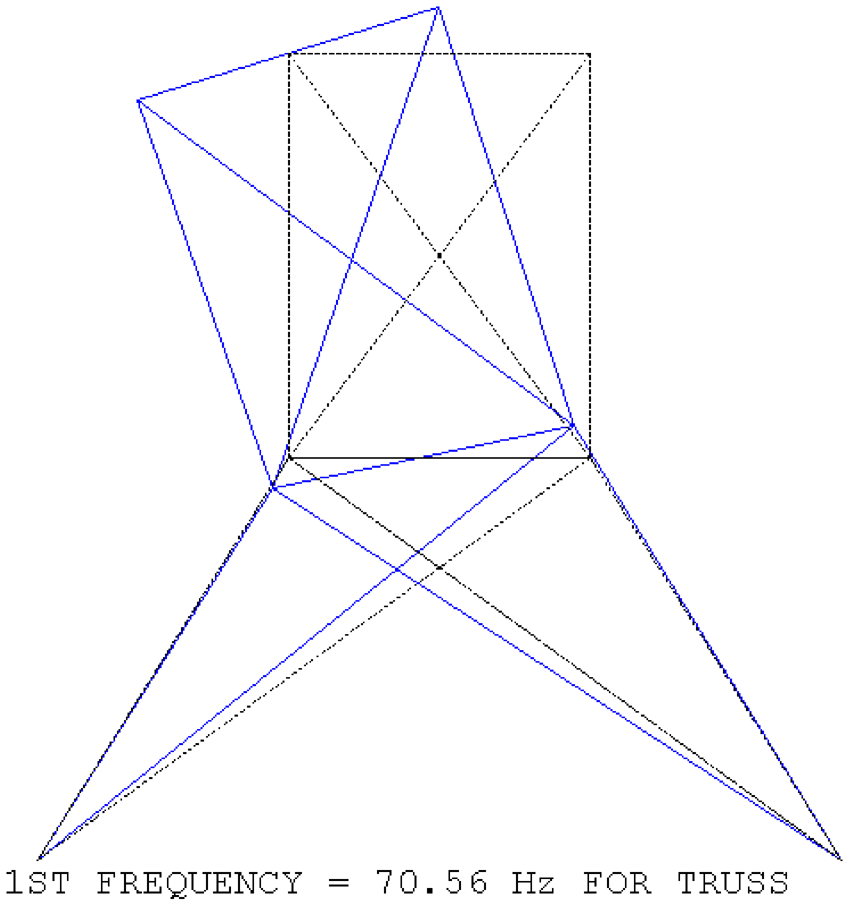

I – pin-joint model

f=70.56 Hz

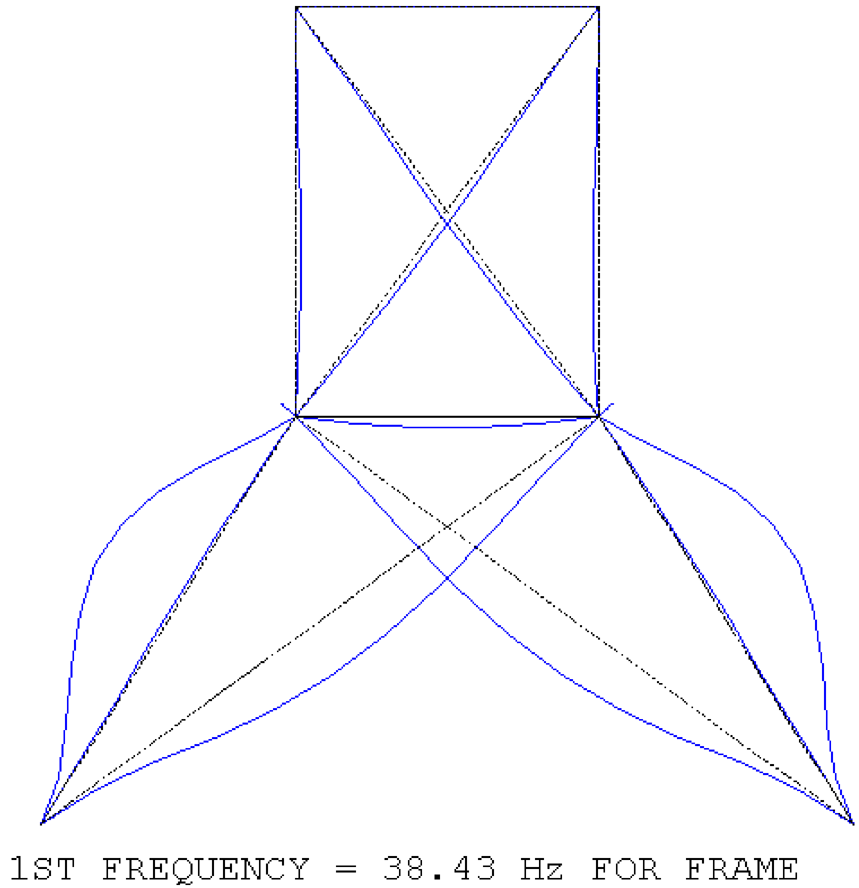

II – rigid-joint model

f=38.43 Hz

First mode shape visualization

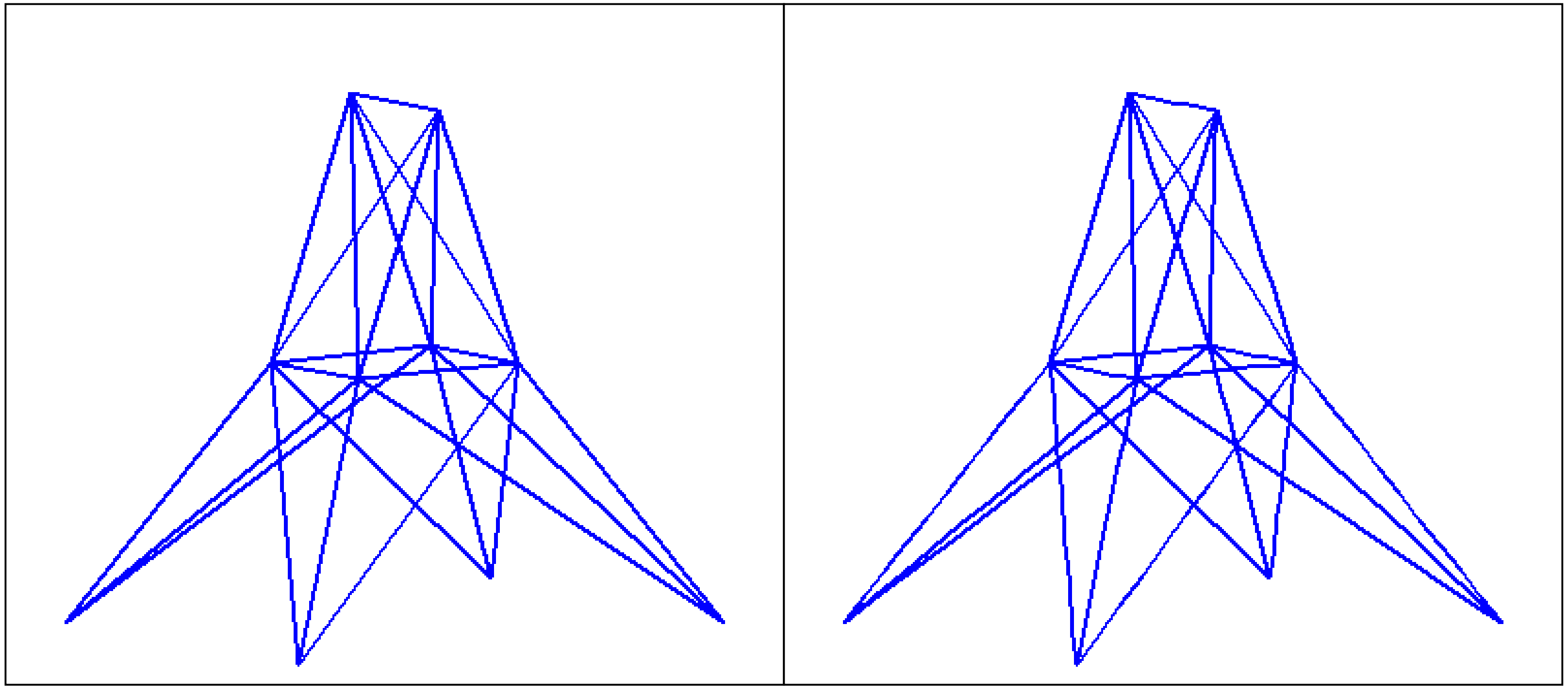

I – pin-joint model

f=70.56 Hz

II – rigid-joint model

f=38.43 Hz

Second mode shape

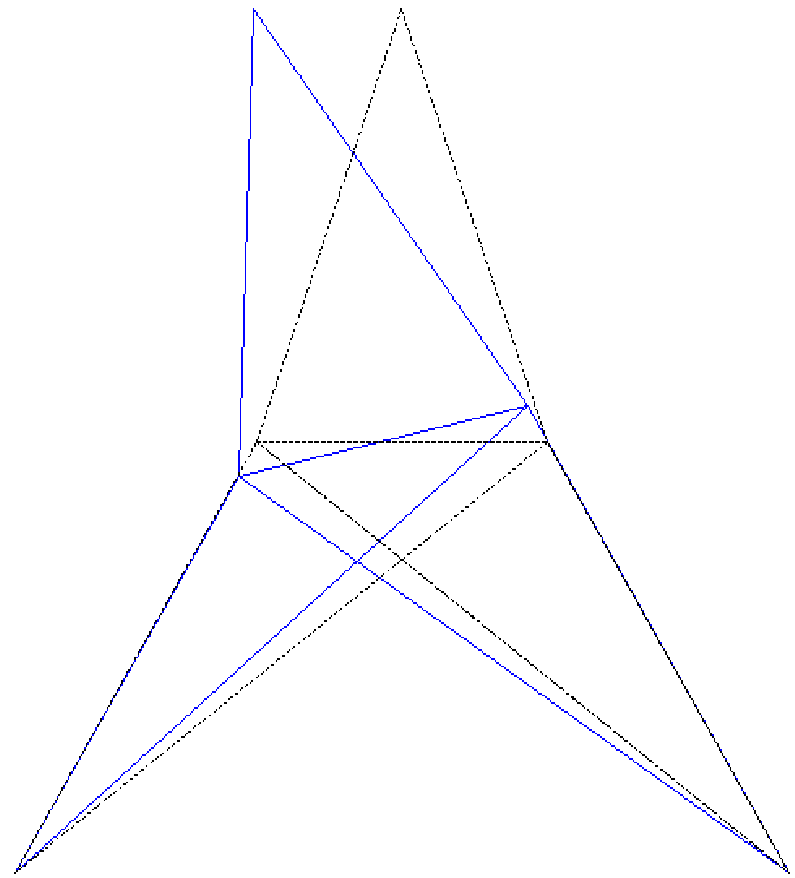

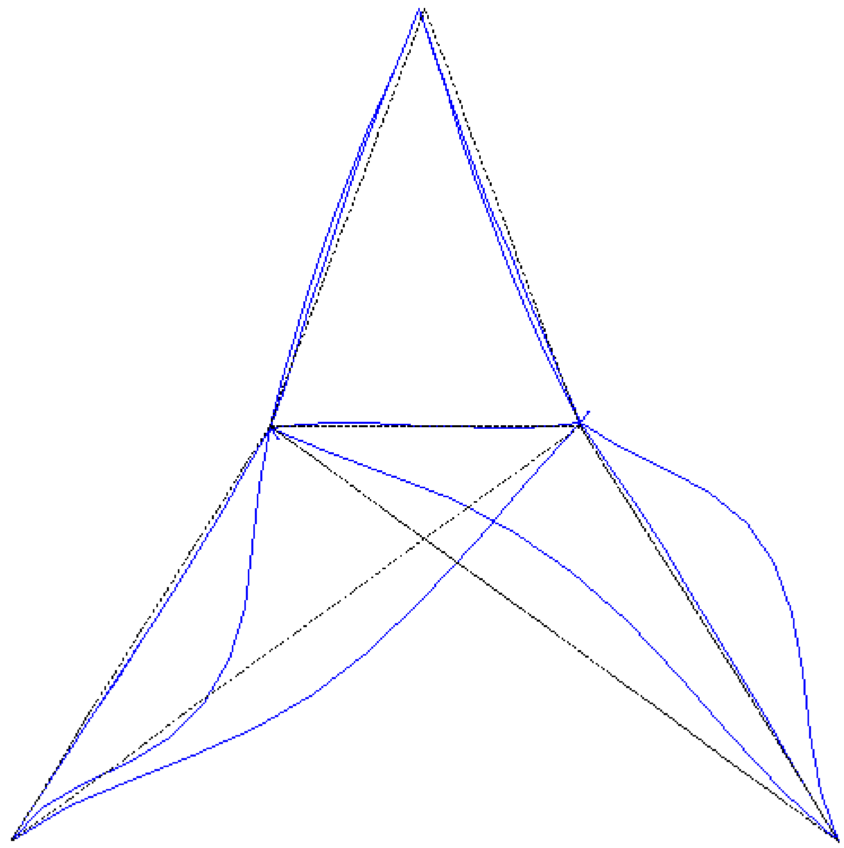

I – pin-joint model

f=73.63 Hz

II – rigid-joint model

f=39.90 Hz

Analytical versus experimental

Computational structural dynamics

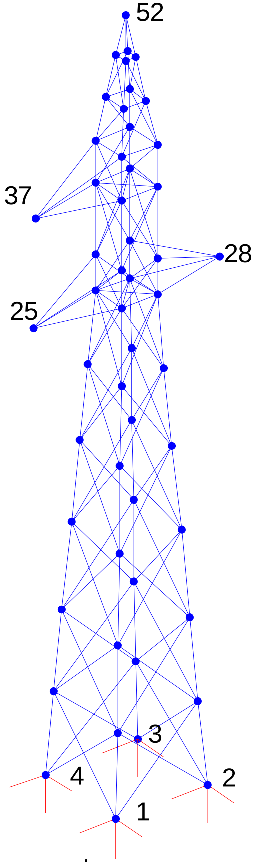

Experimental modal analysis

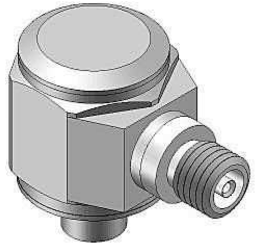

$$\mathbf{M}\ddot{\mathbf{q}} + \mathbf{C}_0\dot{\mathbf{q}} + \mathbf{K}\mathbf{q} = \mathbf{B}_0\mathbf{f}$$

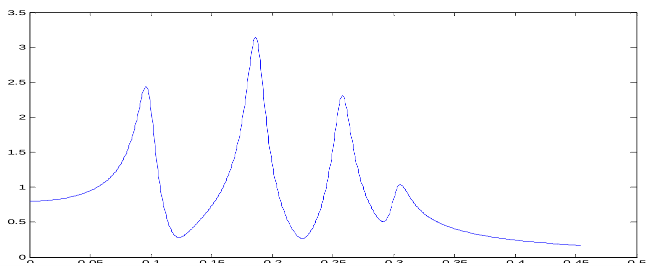

Analytical modal analysis

Equations of motion

Input

$$\mathbf{M}\ddot{\mathbf{q}}(t) + \mathbf{C_0}\dot{\mathbf{q}}(t) + \mathbf{K}\mathbf{q}(t) = \mathbf{B_0}\mathbf{f}(t)$$

Output

$$\mathbf{y}(t) = \mathbf{C_q}\mathbf{q}(t) + \mathbf{C_v}\dot{\mathbf{q}}(t) + \mathbf{C_a}(t)$$

Modal transformation

$$\mathbf{q}(t) = \phi\eta(t)$$

Modal model

$$\ddot{\eta}_i(t) + 2\xi_i\omega_i\dot{\eta}_i(t) + \omega_i^2\eta_i(t) = 0$$

Frequency response function (FRF)

$$\alpha(\omega) = \sum_{i=1}^{n} \frac{\mathbf{C_q}\phi_i\phi_i^T\mathbf{B_0}}{\omega_i^2 + 2\zeta_i\omega_i j\omega - \omega^2}$$

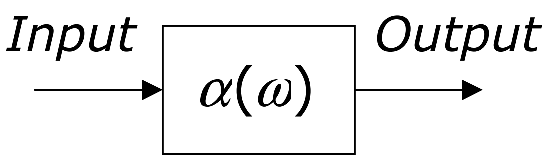

Prefabricated joint – spring model

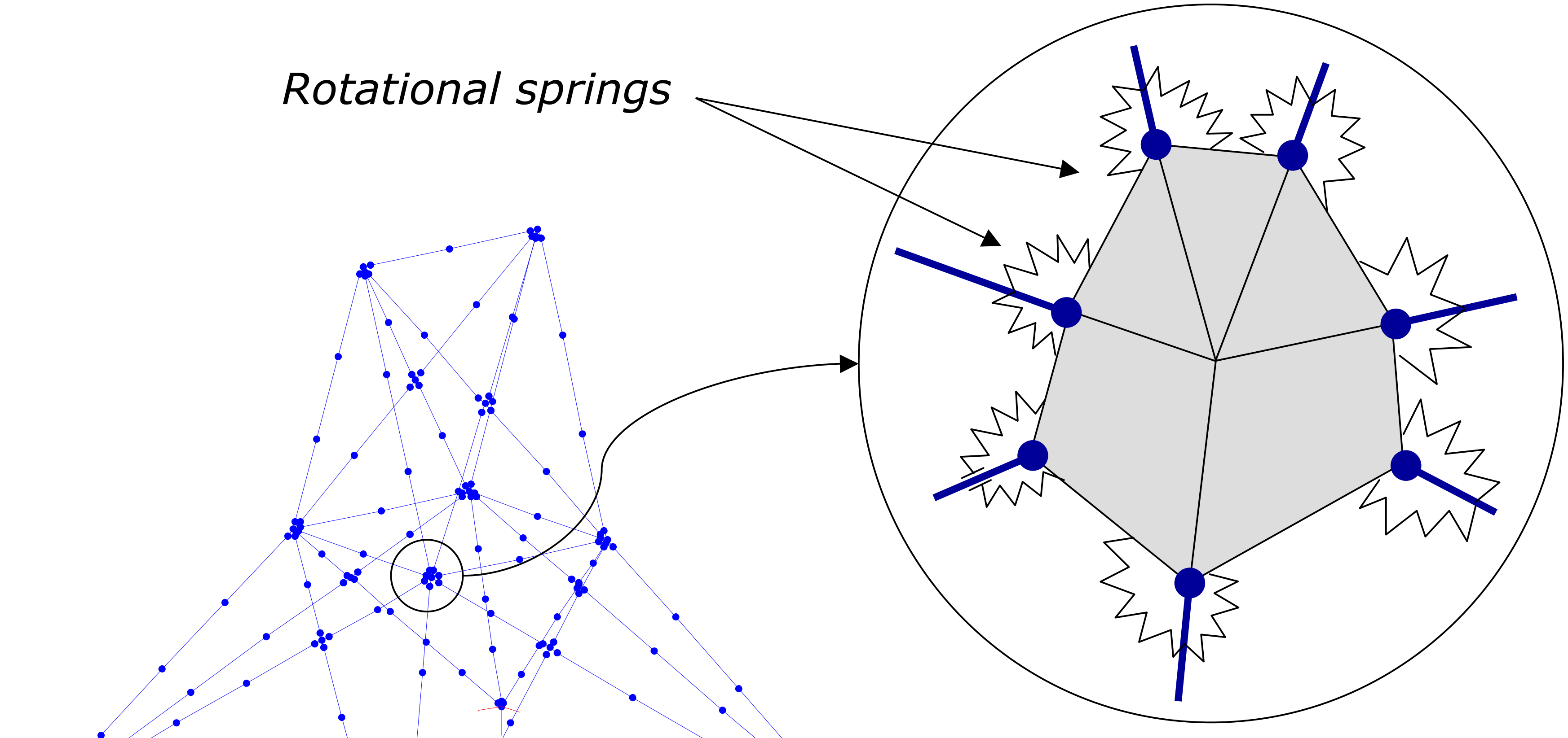

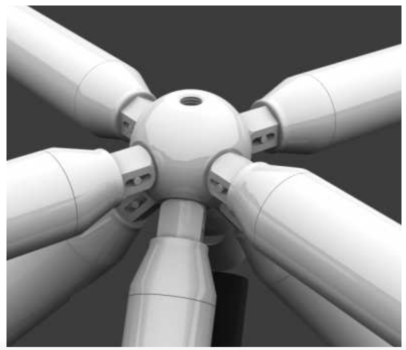

Inverse Eigensensitivity Method

Sensitivities of the eigenvalues

$$\frac{\partial \lambda_r}{\partial p_k} = \{\phi_a\}_r^T \frac{\partial \mathbf{K}}{\partial p_k} \{\phi_e\}_r - (\lambda_e)_r \{\phi_a\}_r^T \frac{\partial \mathbf{M}}{\partial p_k} \{\phi_e\}_r$$

Sensitivities of the eigenvectors

$$\frac{\partial \phi_r}{\partial p_k} = \sum_{i=1, i \neq r}^{N} \frac{\{\phi_a\}_r \{\phi_a\}_r}{(\lambda_e)_r - (\lambda_a)_r} \left[\frac{\partial \mathbf{K}}{\partial p_k} - (\lambda_e)_r \frac{\partial \mathbf{M}}{\partial p_k} \right] \{\phi_e\}_r - \frac{1}{2} \{\phi_a\}_r \{\phi_a\}_r^T \frac{\partial \mathbf{M}}{\partial p_k} \{\phi_e\}_r$$

p_k - *rotational k-th spring stiffness*

$(\lambda_e)_r$, $\{\phi_e\}_r$ - *experimental r-th eigenvalue and eigenvector*

$(\lambda_a)_r$, $\{\phi_a\}_r$ - *analytical r-th eigenvalue and eigenvector*

Inverse Eigensensitivity Method - continued

Taylor series expansion of eigenvalue

$$\lambda_r(\mathbf{p}) = \lambda_r(\mathbf{p_0}) + \sum_{j=1}^{Np} \frac{\partial \lambda_r}{\partial p_j} \Delta p_j + \textit{ higher order terms}$$

Set of simultaneous algebraic equations

$$\begin{bmatrix} \partial\lambda_1/\partial p_1 & \partial\lambda_1/\partial p_2 & \cdots & \partial\lambda_1/\partial p_{Np} \\ \partial\phi_1/\partial p_1 & \partial\phi_1/\partial p_2 & \cdots & \partial\phi_1/\partial p_{Np} \\ \vdots & \vdots & \vdots & \vdots \\ \partial\lambda_m/\partial p_1 & \partial\lambda_m/\partial p_2 & \cdots & \partial\lambda_m/\partial p_{Np} \\ \partial\phi_m/\partial p_1 & \partial\phi_m/\partial p_2 & \cdots & \partial\phi_m/\partial p_{Np} \end{bmatrix} \begin{bmatrix} \Delta p_1 \\ \Delta p_2 \\ \vdots \\ \Delta p_{Np} \end{bmatrix} = \begin{bmatrix} (\lambda_e)_1 - (\lambda_a)_1 \\ \{\phi_e\}_1 - \{\phi_a\}_1 \\ \vdots \\ (\lambda_e)_m - (\lambda_a)_m \\ \{\phi_e\}_m - \{\phi_a\}_m \end{bmatrix}$$

Example 1 – joint stiffness identification

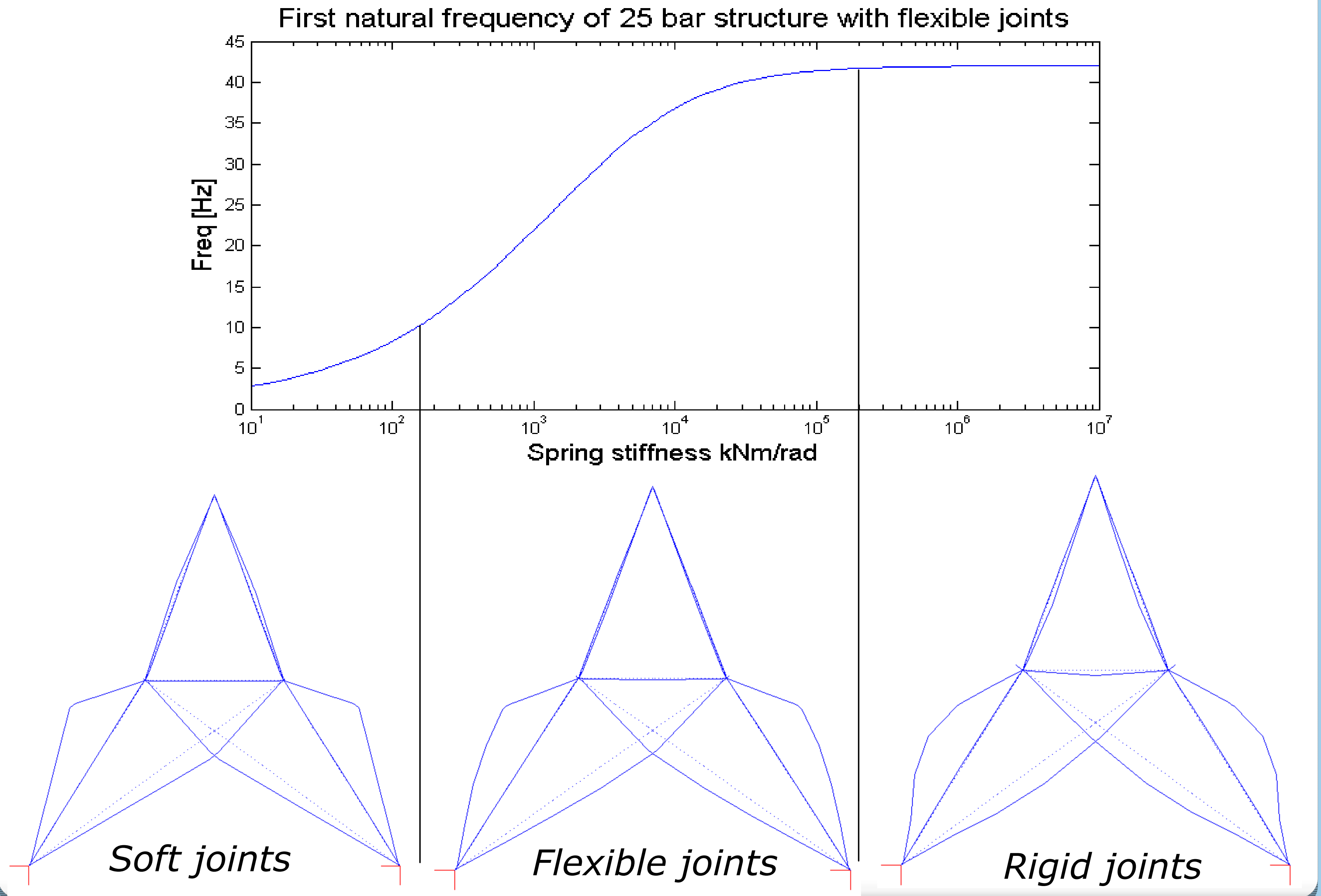

Example 1 - continued

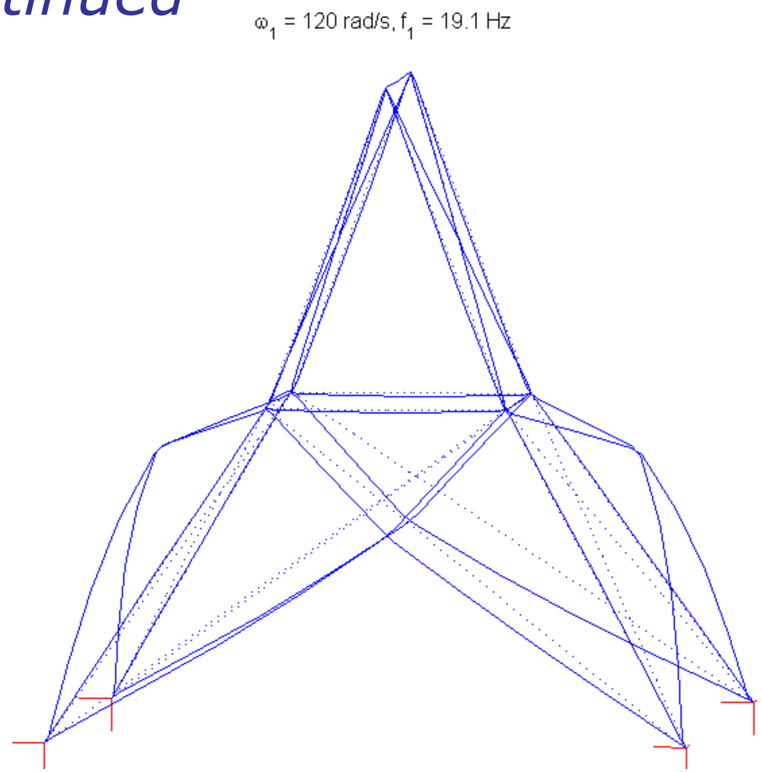

First mode - flexible joints

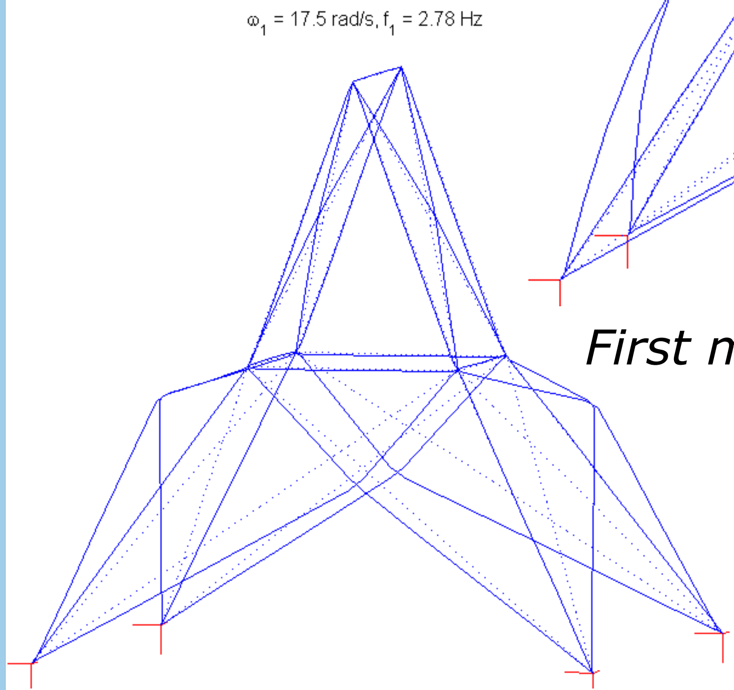

First mode - soft joints

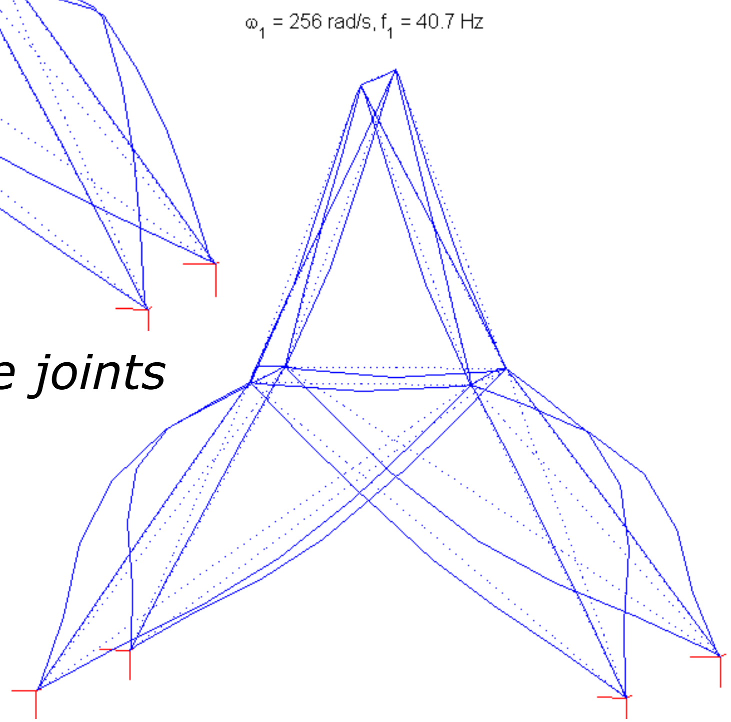

First mode - rigid joints

Example 1 continued

Stiffness sensitivity matrix $\frac{\partial \mathbf{K}}{\partial p}$

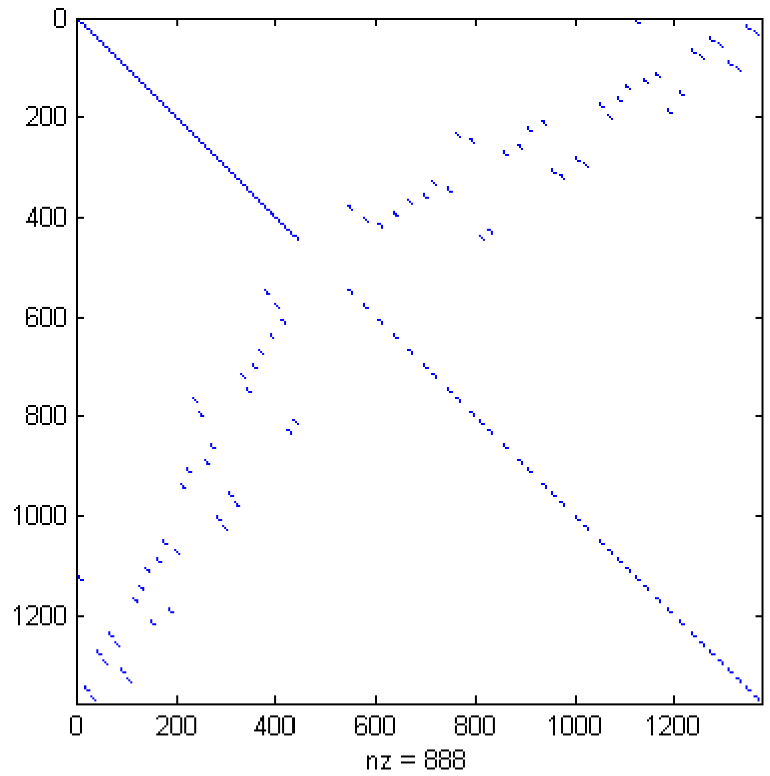

Number of degrees of freedom (DOFs) = 1374

Number of spring elements = 74

Designed joint stiffness p_{design}*=2000 kNm/rad*

Given following measurements

f_{design}[Hz]	$f_{measured}$[Hz]	*difference*
27.08	21.86	19.27%
28.77	23.19	19.36%

we are looking for joint stiffness

After 3 iterations it was found $p_{measured}$*=999.86 kNm/rad*

Example 2 – one joint with reduced stiffness

Modal Assurance Criterion (MAC)

$$MAC(\phi_e, \phi_a) = \frac{\phi_e^T \phi_a}{|\phi_e||\phi_a|}$$

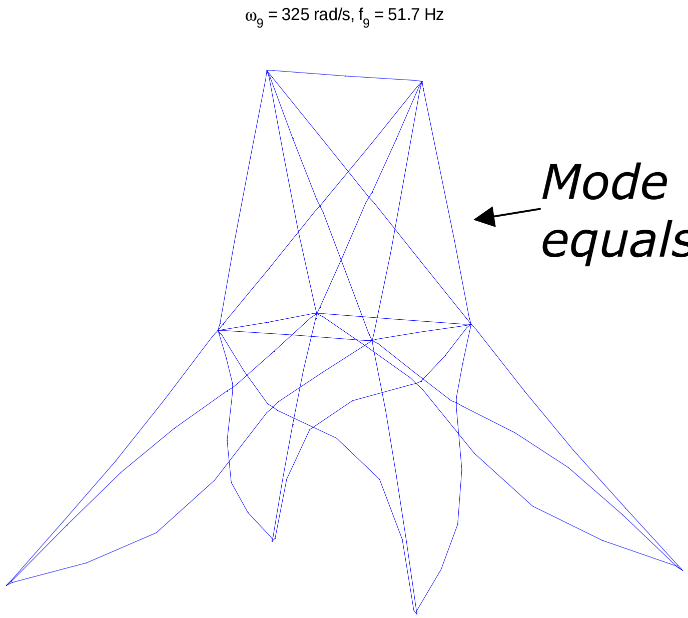

*Mode 9 - joints stiffness equals 2*10³kNm/rad*

Mode	MAC
1	0.9821
2	0.8045
3	0.8043
4	0.9705
5	1.0000
6	0.9999
7	0.5382
8	0.5320
9	0.0043
10	0.0172

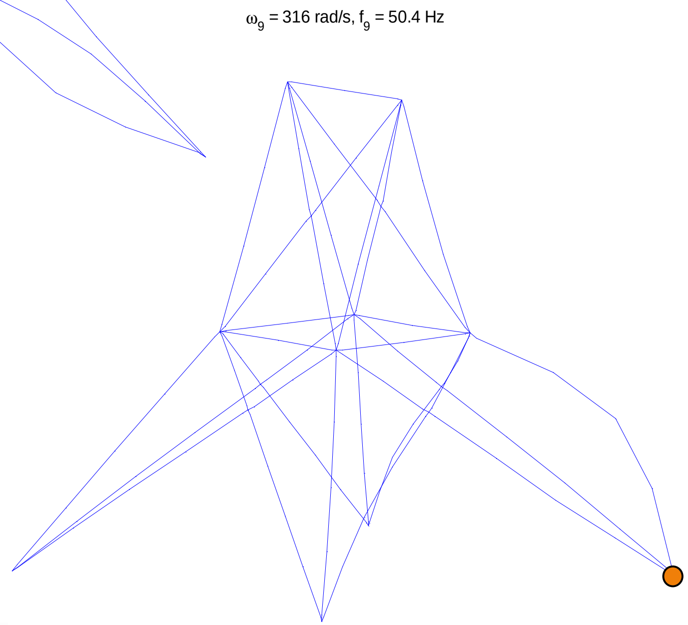

Mode 9

*Joint with stiffness equal to 1*10³ kNm/rad*

Example 2 - continued

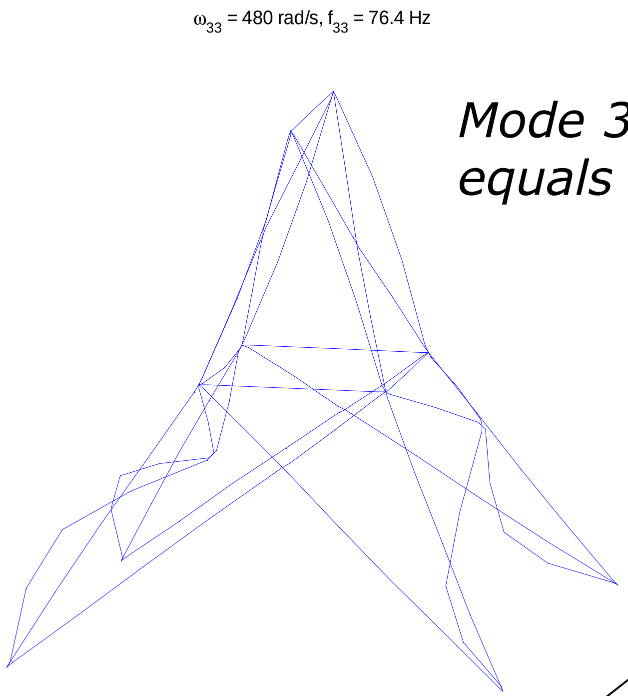

*Mode 33 - joints stiffness equals 2*10³kNm/rad*

Mode	MAC
1	0.9999
2	1.0000
3	1.0000
4	1.0000
5	0.9997
6	0.9994
7	1.0000
8	1.0000
9	1.0000
10	1.0000
:	:
<u>33</u>	<u>0.7213</u>

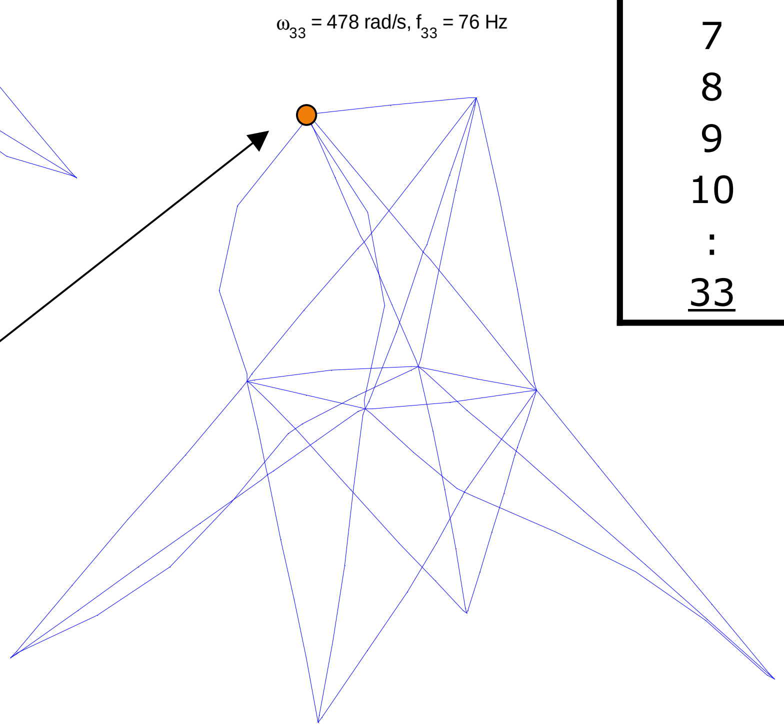

*Joint with reduced stiffness equal to 1*10³ kNm/rad*

Antenna tower

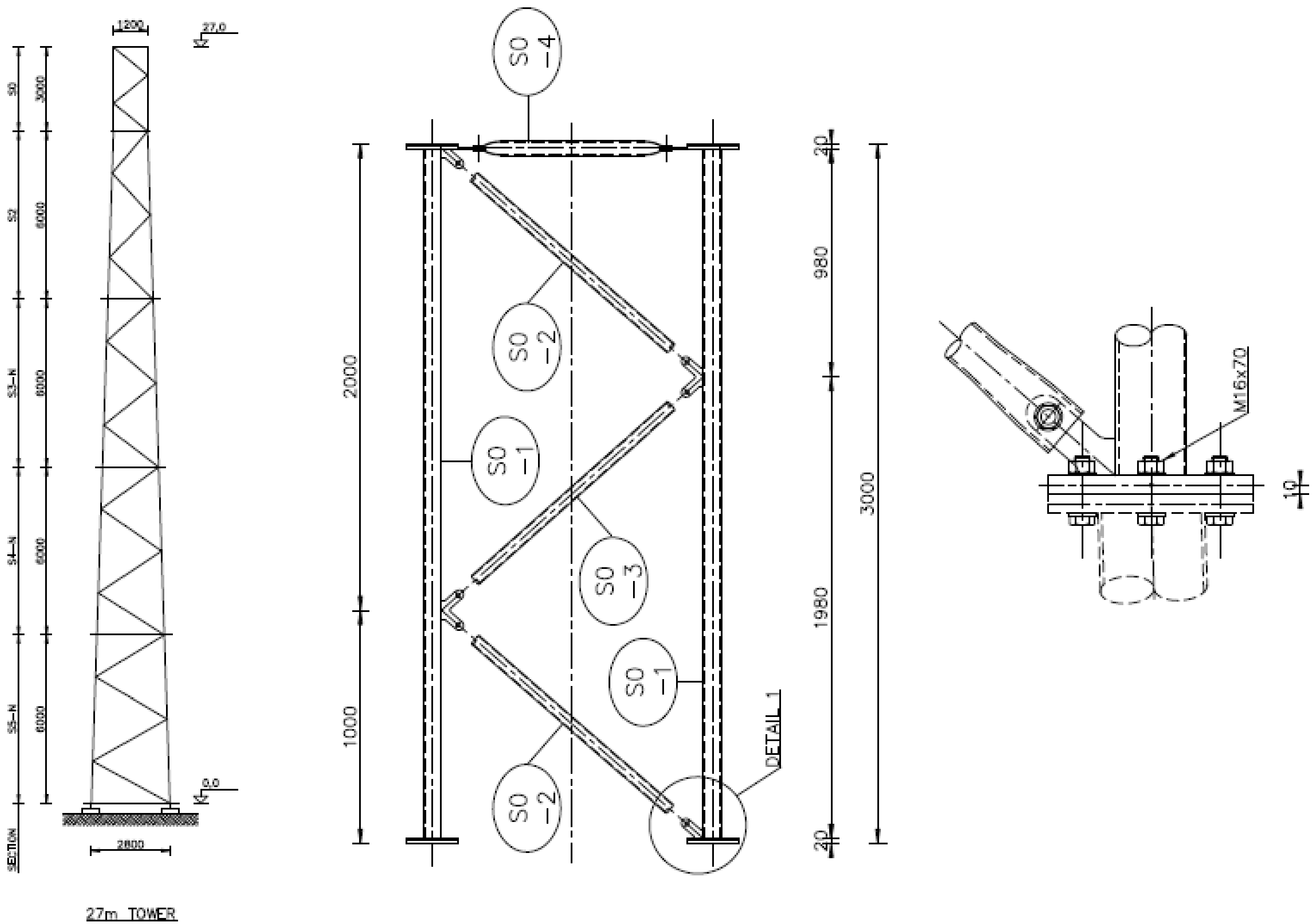

Substructuring in computational structural dynamics

Decomposition of one large structure into Ns substructures

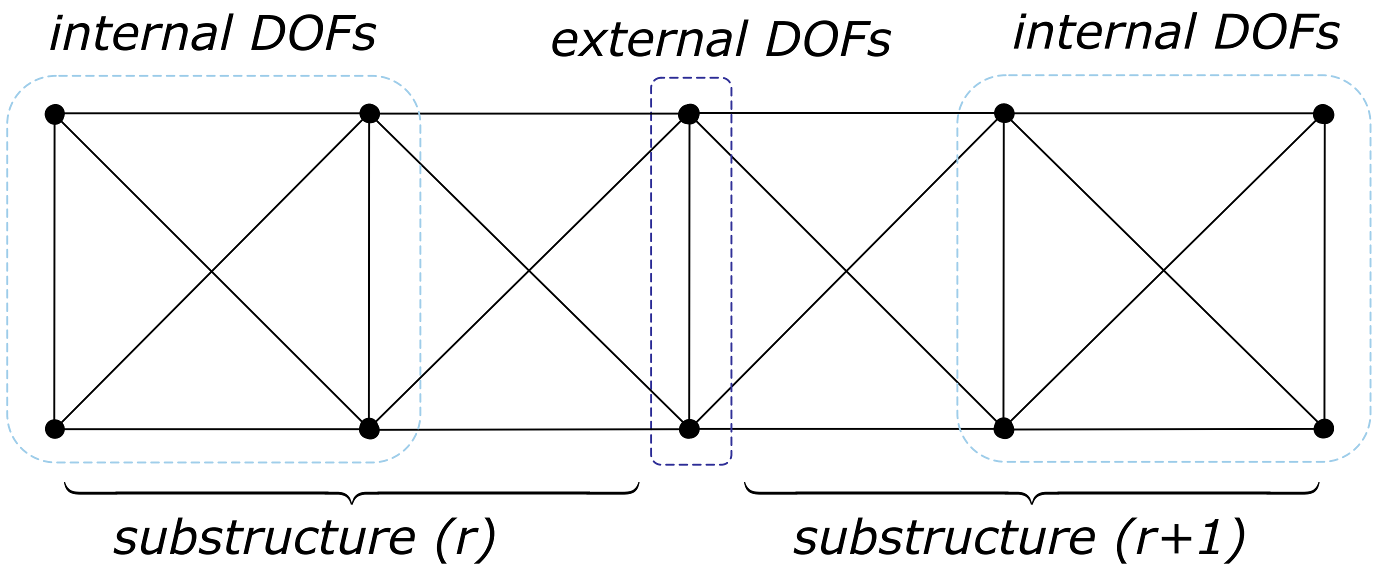

Motion equations of (r)-th substructure:

$$\mathbf{M}^{(r)}\ddot{\mathbf{q}}^{(r)}(t)+\mathbf{K}^{(r)}\mathbf{q}^{(r)}(t)=\mathbf{f}^{(r)}(t)$$

Model reduction techniques in structural dynamics

For each substructure:

$$\begin{bmatrix} \mathbf{M}_{mm}^{(r)} & \mathbf{M}_{ms}^{(r)} \\ \mathbf{M}_{sm}^{(r)} & \mathbf{M}_{ss}^{(r)} \end{bmatrix} \begin{bmatrix} \ddot{\mathbf{q}}_{m}^{(r)} \\ \ddot{\mathbf{q}}_{s}^{(r)} \end{bmatrix} + \begin{bmatrix} \mathbf{K}_{mm}^{(r)} & \mathbf{K}_{ms}^{(r)} \\ \mathbf{K}_{sm}^{(r)} & \mathbf{K}_{ss}^{(r)} \end{bmatrix} \begin{bmatrix} \mathbf{q}_{m}^{(r)} \\ \mathbf{q}_{s}^{(r)} \end{bmatrix} = \begin{bmatrix} \mathbf{f}_{m}^{(r)} \\ \mathbf{f}_{s}^{(r)} \end{bmatrix}$$

m - master (external) degrees of freedom

s - slave (internal) degrees of freedom

Guyan reduction

$$\begin{bmatrix} \mathbf{q}_{m}^{(r)} \\ \mathbf{q}_{s}^{(r)} \end{bmatrix} = \begin{bmatrix} \mathbf{I} \\ -\left(\mathbf{K}_{ss}^{(r)}\right)^{-1} \mathbf{K}_{sm}^{(r)} \end{bmatrix} \mathbf{q}_{m}^{(r)} = \mathbf{T}^{(r)} \mathbf{q}_{m}^{(r)}$$

Craig-Bampton component mode synthesis

$$\begin{bmatrix} \mathbf{q}_{m}^{(r)} \\ \mathbf{q}_{s}^{(r)} \end{bmatrix} = \begin{bmatrix} \mathbf{I} & \mathbf{0} \\ -\left(\mathbf{K}_{ss}^{(r)}\right)^{-1} \mathbf{K}_{sm}^{(r)} & \phi^{(r)} \end{bmatrix} \begin{bmatrix} \mathbf{q}_{m}^{(r)} \\ \eta^{(r)} \end{bmatrix} = \mathbf{T}^{(r)} \mathbf{q}_{CMS}^{(r)}$$

Substructuring continued

Substituting Craig-Bampton transformation

$$\left(\mathbf{T}^{(r)}\right)^T \mathbf{M}^{(r)} \mathbf{T}^{(r)} \ddot{\mathbf{q}}^{(r)}(t) + \left(\mathbf{T}^{(r)}\right)^T \mathbf{K}^{(r)} \mathbf{T}^{(r)} \mathbf{q}^{(r)}(t) = \left(\mathbf{T}^{(r)}\right)^T \mathbf{f}^{(r)}(t)$$

Reduced motion equations of (r)-th substructure

$$\hat{\mathbf{M}}^{(r)} \ddot{\hat{\mathbf{q}}}^{(r)}(t) + \hat{\mathbf{K}}^{(r)} \hat{\mathbf{q}}^{(r)}(t) = \hat{\mathbf{f}}^{(r)}(t)$$

Assembling substructures into global matrices of structure

$$\hat{\mathbf{M}} = \sum_{r=1}^{Ns} \left(\mathbf{P}^{(r)}\right)^T \hat{\mathbf{M}}^{(r)} \mathbf{P}^{(r)}$$

$$\hat{\mathbf{K}} = \sum_{r=1}^{Ns} \left(\mathbf{P}^{(r)}\right)^T \hat{\mathbf{K}}^{(r)} \mathbf{P}^{(r)}$$

$\mathbf{P}^{(r)}$ - *boolean matrices*

Reduced motion equations of whole structure

$$\hat{\mathbf{M}} \ddot{\hat{\mathbf{q}}}(t) + \hat{\mathbf{K}} \hat{\mathbf{q}}(t) = \hat{\mathbf{f}}(t)$$

Tubular welded joint

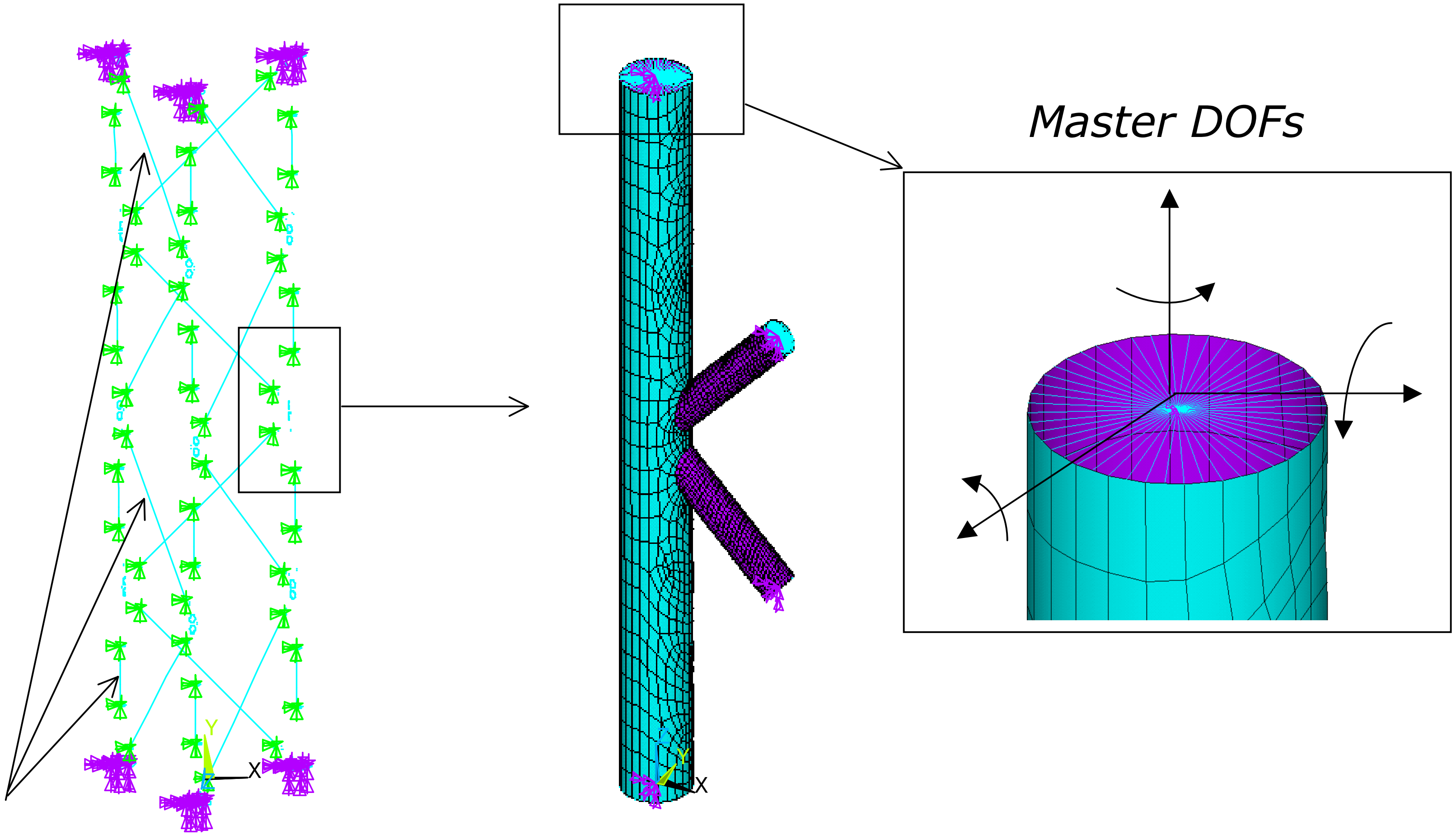

Classical beam elements

Joint superelement

Flanged bolted joint

Leg

CHS 101.6/8 mm

Joint flange

25 mm thickness

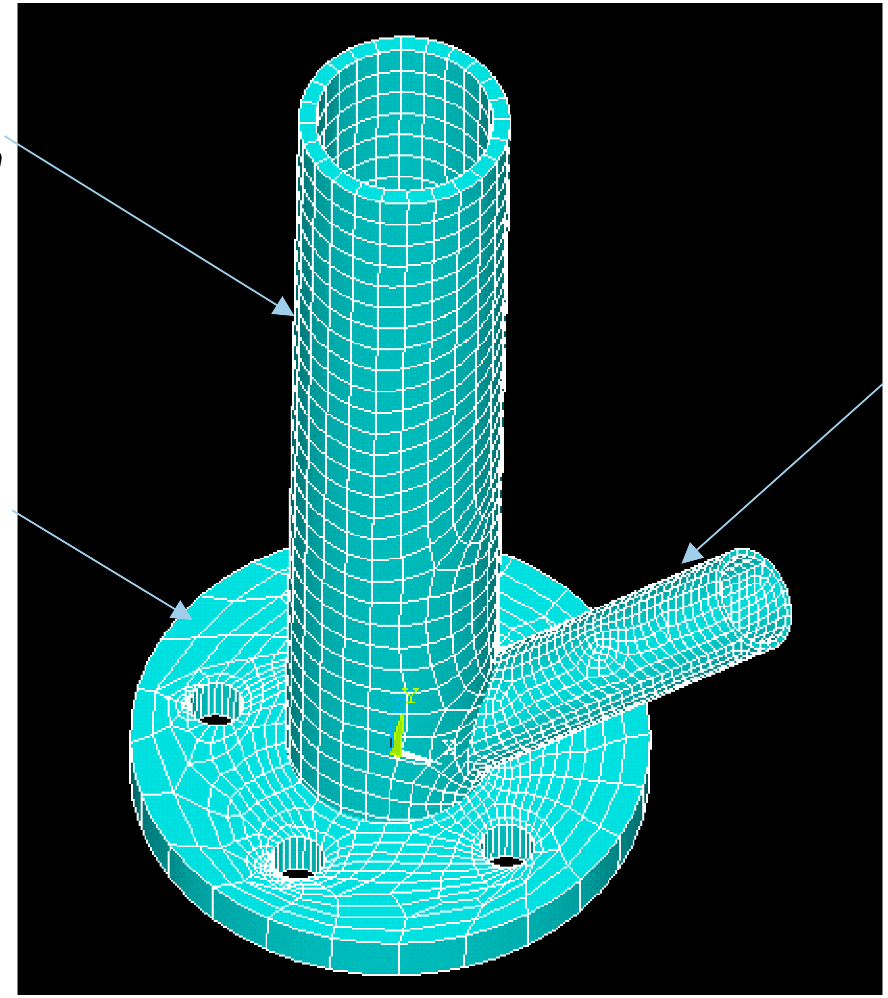

Diagonals

CHS 51/3.2 mm

Flanged bolted joint - continued

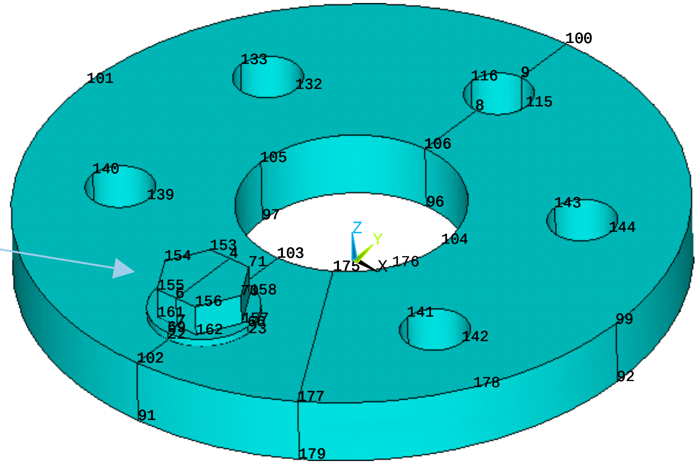

Structural bolts M24

Symmetry boundary condition

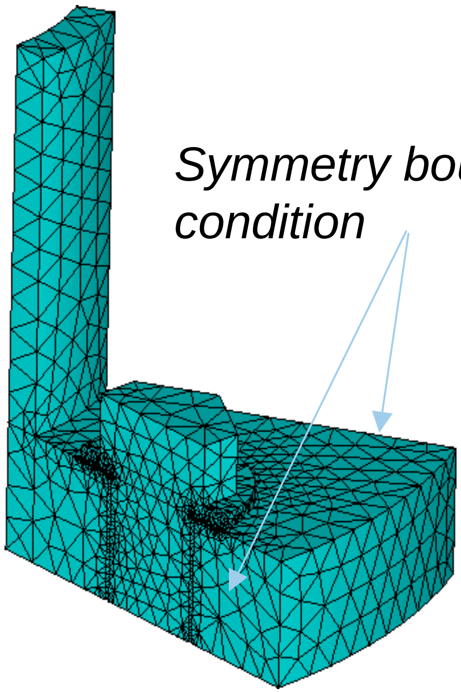

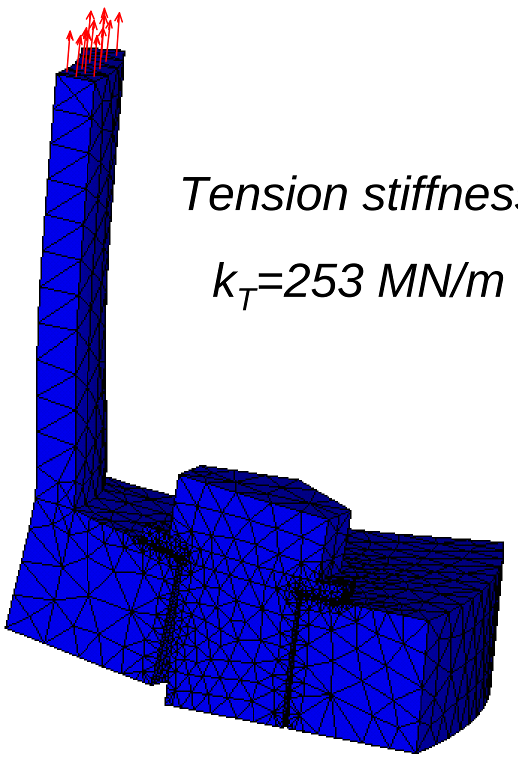

Tension stiffness

k_T=253 MN/m

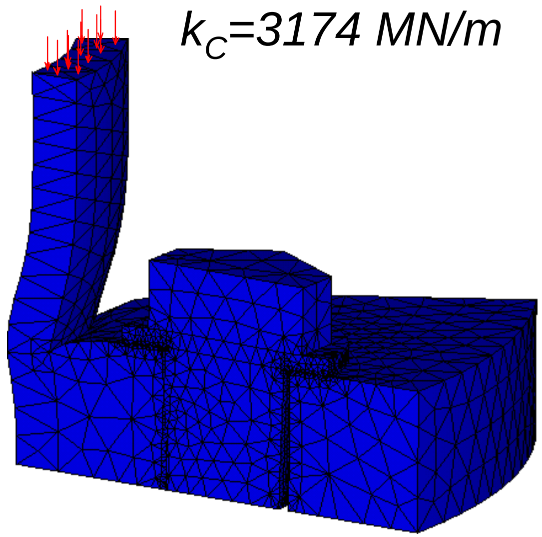

Compression stiffness

k_C=3174 MN/m

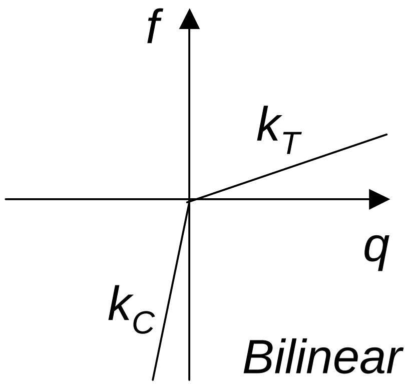

Bilinear characteristic

System identification in experimental modal analysis

Frequency domain methods

Peak picking – SDOF method

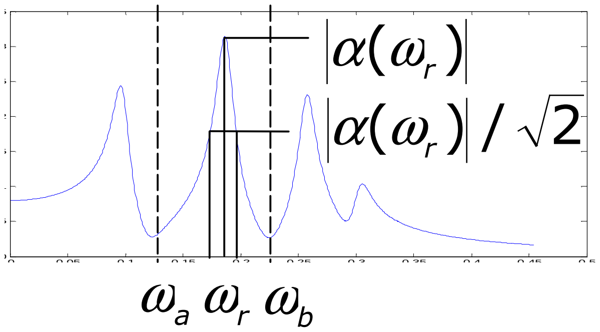

Damping coefficient

$$\xi_r = \frac{\omega_b - \omega_a}{2\omega_r}$$

Modal constant

$$A_r = 2|\alpha(\omega_r)|\xi_r\omega_r^2$$

Time domain methods

Ibrahim time domain method

$$\mathbf{M}\ddot{\mathbf{q}}(t) + \mathbf{C_0}\dot{\mathbf{q}}(t) + \mathbf{K}\mathbf{q}(t) = \mathbf{0}$$

$$\begin{bmatrix} \dot{\mathbf{q}} \\ \ddot{\mathbf{q}} \end{bmatrix} = \begin{bmatrix} \mathbf{0} & \mathbf{I} \\ -\mathbf{M}^{-1}\mathbf{K} & -\mathbf{M}^{-1}\mathbf{C}_0 \end{bmatrix} \begin{bmatrix} \mathbf{q} \\ \dot{\mathbf{q}} \end{bmatrix}$$

$$\mathbf{y}(t) = \begin{bmatrix} \mathbf{q}(t) \\ \dot{\mathbf{q}}(t) \end{bmatrix}$$

$$\dot{\mathbf{y}}(t) = \mathbf{A}\mathbf{y}(t)$$

$$\mathbf{Y} = \begin{bmatrix} \mathbf{q}(t_1) & \mathbf{q}(t_2) & \dots & \mathbf{q}(t_{Ny}) \\ \dot{\mathbf{q}}(t_1) & \dot{\mathbf{q}}(t_2) & \dots & \dot{\mathbf{q}}(t_{Ny}) \end{bmatrix}$$

$$\mathbf{A} = \dot{\mathbf{Y}}\mathbf{Y}^{-1}$$

Structural Dynamics Toolbox for 3D Frames

Modules

CAD Translators:
- -Import DXF format
- -Import, export txt files from ANSYS

Sensitivity based ID:
- -Inverse Eigensensitivity Method

Modal parametrs ID:
- -Peak Picking Method
- -Ibrahim time domain
- -Random decrement

Substructuring:
- -3D beam element
- -Spring model of semi-rigid joints
- -Guyan reduction

Wnioski

- Zweryfikowano statyczne założenia przegubowego połączenia elementów w układach prętowych dla przypadku drgań. Wykazano, że przenoszenie założeń statycznych do dynamiki może prowadzić do błędów

- Wykorzystano analizę wrażliwości parametrów modalnych do oceny sztywności połączeń w konstrukcjach prętowych z uwzględnieniem rzeczywistej postaci węzłów

Wnioski cd.

- Do modelowania złożonych węzłów monolitycznych wykorzystano technikę „*substructuring*". Przedstawiono przykład spawanego połączenia rurowego oraz połączenia kołnierzowego

- Zaimplementowano podstawowe procedury numeryczne do analizy dynamicznej konstrukcji prętowych o węzłach podatnych

Dziękuję za uwagę!